

Supporting Information

Materials and Orthopedic Applications for Bioresorbable Inductively Coupled Resonance Sensors

Aleksi Palmroth^{a,*}, Timo Salpavaara^a, Petri Vuoristo^b, Sanna Karjalainen^a, Tommi Kääriäinen^{c,†}, Susanna Miettinen^a, Jonathan Massera^a, Jukka Leikkala^a, Minna Kellomäki^a

^aBioMediTech, Faculty of Medicine and Health Technology, Tampere University. Korkeakoulunkatu 3, Tampere 33720, Finland.

^bMaterials Science and Environmental Engineering, Faculty of Engineering and Natural Sciences, Tampere University. Korkeakoulunkatu 6, Tampere 33720, Finland.

^cDepartment of Chemistry, University of Colorado, Boulder, Colorado 80309, United States.

*Corresponding author: aleksi.palmroth@tuni.fi

Contents

1. Cell culture results and discussion (Figure S1)
2. Cell culture methods
3. Skin depths of common bioresorbable metals (Table S1)
4. Corrosion testing of magnesium films (7.5 μm) (Figure S2)
5. In vitro degradation photographs of the wireless Mg and Zn pressure sensors (Figure S3)
6. Molybdenum wire immersion test (Figure S4)
7. Illustration of the peeled-off area of the ALD coatings (Figure S5)
8. ALD coated substrates in an LC resonator
9. References

1. Cell culture results and discussion

The cytotoxicity of PDTEC was evaluated by culturing a human fibroblast cell line (ATCC, CRL-2429) on compression molded discs using standard polystyrene 24-well plates (Nunc, Denmark) as a control and PLDLA 96/4 discs as a bioresorbable reference material. Based on the crystal violet staining (Figure S1a-b), the cell growth on PDTEC was comparable if not superior to the reference materials. The result is in agreement with earlier cell data using rat lung fibroblasts, where the cytotoxicity level of PDTEC was estimated to be comparable to glass and hydrophilic modified polystyrene.¹ The Live/Dead images showed a rather spherical fibroblast shape during the first days of culture (Figure S1c). The alive cells were colored green, whereas no red color (indicating dead cells) were noticed in the images. After 7 days, the amount of elongated cells increased.

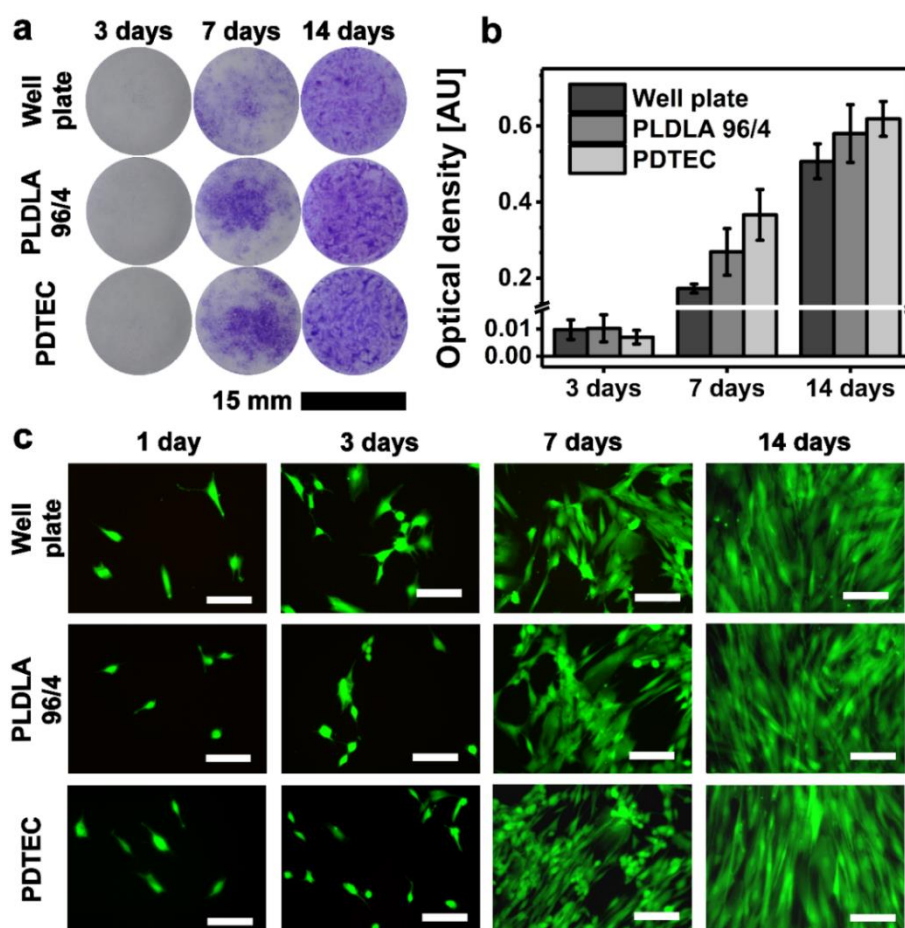


Figure S1. The in vitro cytotoxicity assessment of different materials using (a) Crystal violet staining (b) Quantitative crystal violet staining (n=8), where the bound dye was solubilized in 10 % acetic acid and its optical density in absorbance units (AU) was measured at 590 nm. The optical density correlates to the number of cells. (c) Live/Dead staining where green color depicts alive cells. Dead cells would have been shown in red. The scale bars are 100 μ m.

2. Cell culture methods

PDTEC and PLDLA 96/4 sheets were compression molded against glass to yield a smooth surface. Polymer discs ($\text{\O} = 14$ mm) were punch-cut from the sheets, washed in 2-propanol (VWR Chemicals), dried and sterilized by gamma irradiation (BBF Sterilisationservice GmbH, Kernen im Remstal, Germany) with a minimum dose of 25 kGy.

Human foreskin fibroblasts (ATCC, CRL-2429) at passage 12 were seeded onto the bioresorbable polymer discs as well as directly onto the polystyrene 24-well plates ($\text{\O} = 15$ mm; Nunc, Roskilde, Denmark) by first adding 1 ml of cell culture medium onto each well and then pipetting 1000 cells in 50 μl of cell suspension onto each well. The cell culture medium consisted of DMEM/F-12 (DMEM/F-12 1:1; Gibco by Life Technologies, United Kingdom) supplemented with 10 % fetal bovine serum (FBS; Gibco by Life Technologies), 1 % L-glutamine (GlutaMAX I; Thermo Fischer Scientific, USA) and 1 % antibiotics (100 U/ml penicillin; 100 U/ml streptomycin; Lonza, Switzerland). The fibroblasts were cultured at 37 °C in 5 % CO_2 and the medium was changed twice a week.

The viability of the fibroblasts was evaluated with Live/Dead staining probes (Invitrogen Molecular Probes, USA) after 1, 3, 7 and 14 days of culture.² The fibroblasts were incubated in 0.25 mM EthD-1 (Molecular Probes) and 0.5 mM calcein AM (Molecular Probes) in Dulbecco's Phosphate Buffered Saline (DPBS; Sigma Aldrich, United Kingdom) for 45 minutes and then imaged with a phase-contrast microscope (Olympus IX51, Japan) with fluorescence optics. The fibroblast imaging was done by transferring the bioresorbable substrate discs onto clean well plates, whereas well plate controls were imaged directly from the polystyrene wells.

The relative cell number was determined with a quantitative crystal violet staining method with slight modifications.³ The fibroblasts were fixed onto their substrates with 5% glutaraldehyde in 0.1 M PBS. The washed and dried substrates were then incubated for 20 minutes with 250 μl of 0.1 % crystal violet stain (Merck) in H_2O (milli-Q). The fibroblasts were then washed with H_2O until the washing solution was clear, after which the substrates were allowed to dry. The samples were then photographed before solubilizing the dye bound in the cell nuclei in 10 % acetic acid (J.T. Baker, Deventer, the Netherlands). The amount of acetic acid was calculated based on the substrate culture area, using 550 μl for the reference wells ($\text{\O} = 15$ mm) and 480 μl for the bioresorbable polymer discs ($\text{\O} = 14$ mm).⁴ The optical density (590 nm) was measured from each well using Victor 1420 multilabel plate reader (Wallac, Turku, Finland). This resulted in relative cell numbers given as absorbance units. Eight parallel samples were measured to calculate the mean optical density \pm standard deviation for each

material at each time point. Stained substrates without cells were used as a baseline by subtracting their optical density values from the adjacent time-point measurements (3, 7 and 14 days) containing cells.

3. Skin depths of common biodegradable metals

Table S1 summarizes the skin depth values of the most commonly used biodegradable conductor metals. The values were calculated using the equation:

$$\text{Skin depth } \delta = \sqrt{\frac{\rho}{\pi f \mu_0 \mu_r}}$$

where ρ is the electrical resistivity of the material, f the frequency and μ_0 the permeability constant ($4\pi \times 10^{-7}$ H/m).⁵ The relative permeability μ_r was approximated as 1 for all other metals except for Fe, whose μ_r estimation was 5500.⁶

Table S1. The electrical characteristics of the most common biodegradable metals.

Material	Electrical resistivity at 295 K ($\Omega \times 10^{-8} \text{m}$)	Skin depth @ 10 MHz	Skin depth @ 50 MHz	Skin depth @ 100 MHz	Skin depth @ 500 MHz
Magnesium (Mg)	4.3	33 μm	15 μm	10 μm	5 μm
Zinc (Zn)	5.9	39 μm	17 μm	12 μm	5 μm
Iron (Fe)	9.8	0.7 μm	0.3 μm	0.2 μm	0.01 μm
Molybdenum (Mo)	5.3	37 μm	16 μm	12 μm	5 μm

4. Corrosion testing of magnesium films (7.5 μm)

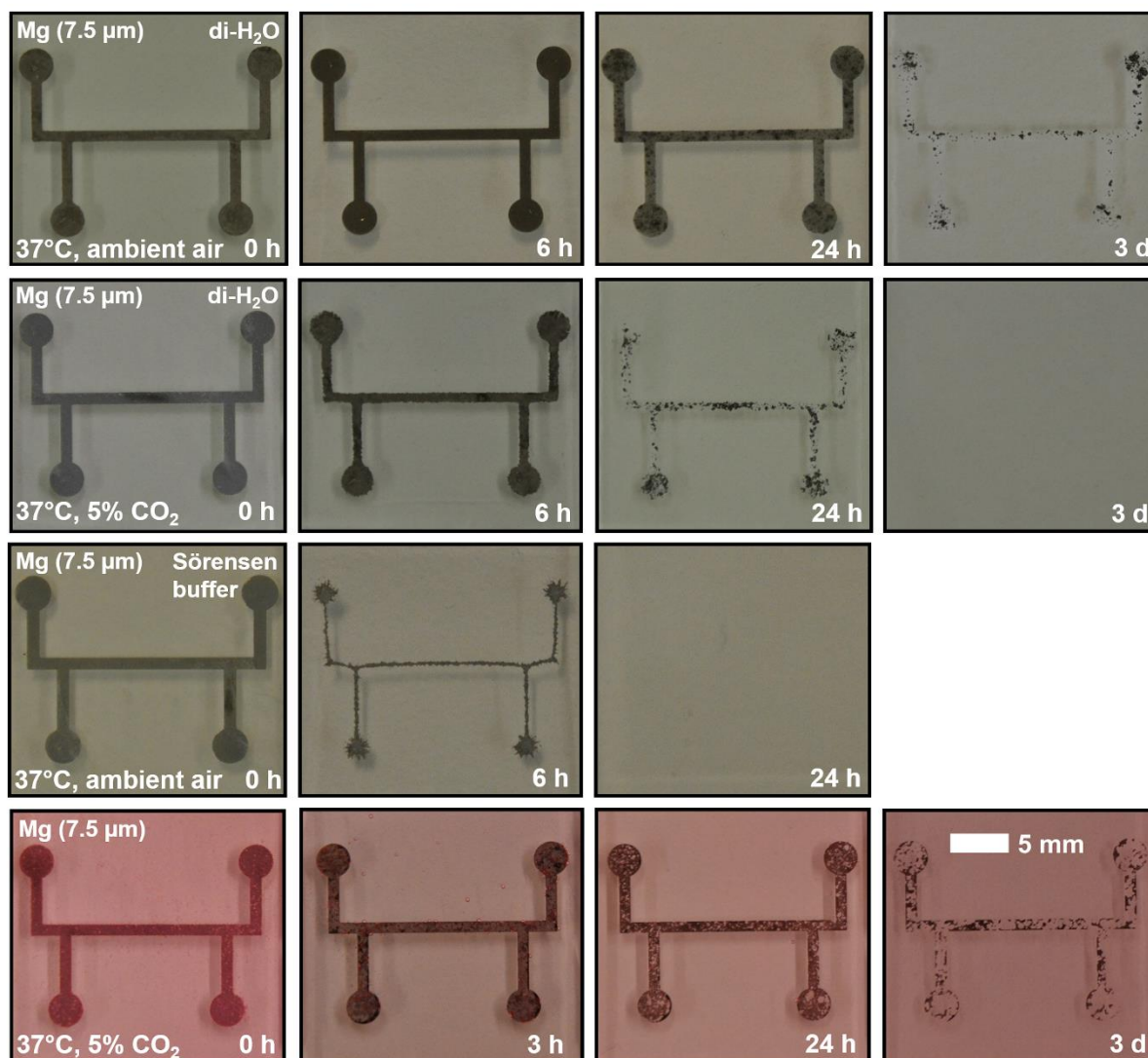


Figure S2. Comparison of the corrosion behavior of Mg films (7.5 μm) in different immersion environments at +37 °C. The undermost row shows samples immersed in cell culture media, which consisted of Minimum Essential Medium supplemented with 10 % FBS and 1 % antibiotics.

5. In vitro degradation photographs of the wireless Mg and Zn pressure sensors

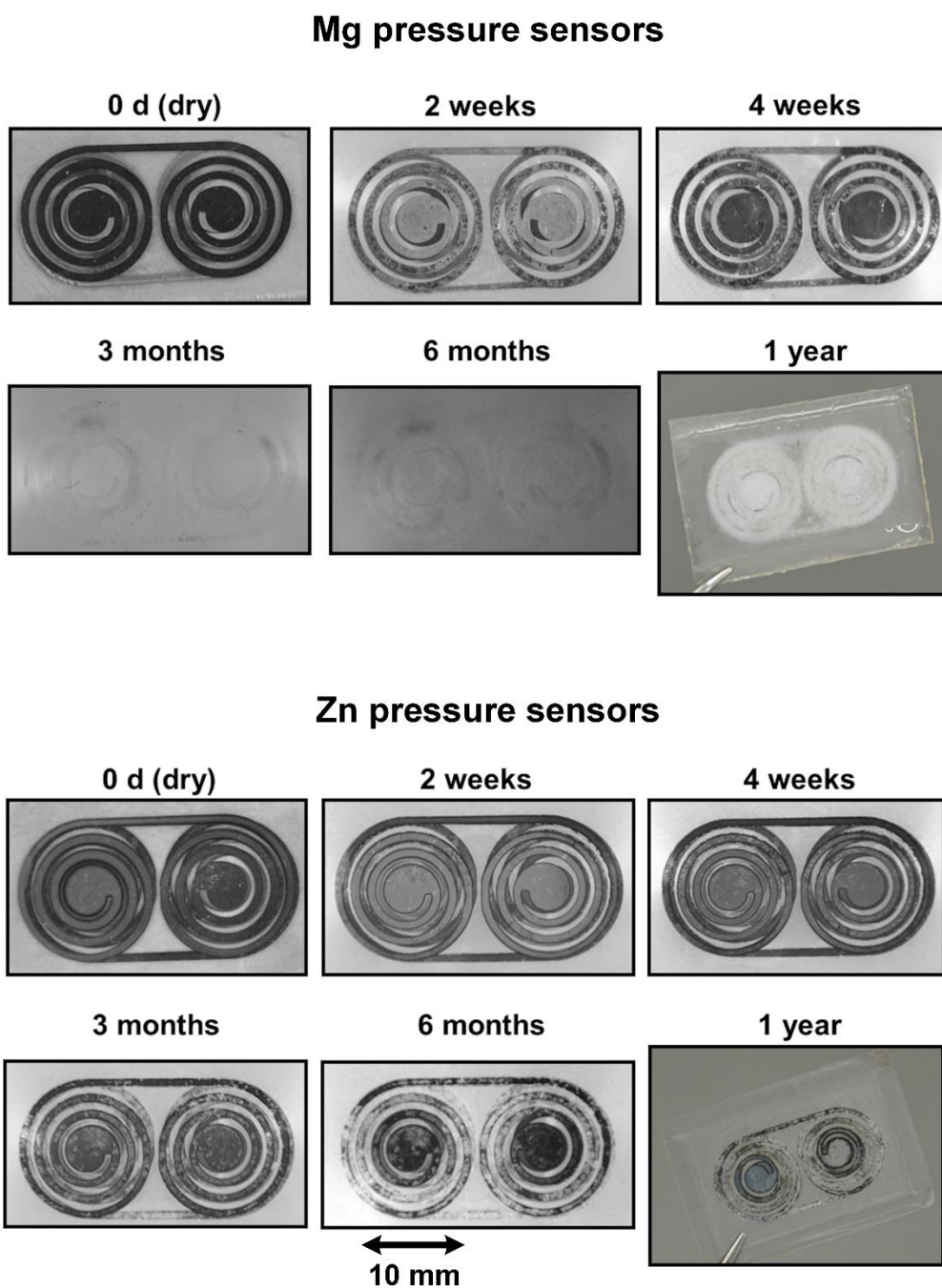


Figure S3. Photographs of the Mg and Zn pressure sensors immersed in Sørensen buffer (+37 °C). The conductors are encapsulated inside the PDTEC substrates as illustrated in the 1-year images.

6. Molybdenum wire immersion test

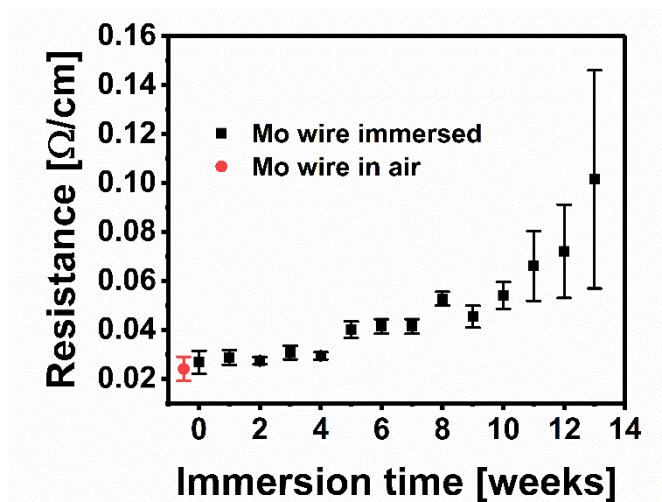


Figure S4. The electrical resistance of uncoated molybdenum wires (200 μm) immersed in Sørensen buffer solution at +37 $^{\circ}\text{C}$. The tips of the 30 cm wires were attached to the lid of 50 ml falcon tubes for reliable non-immersed measurement points.

7. Illustration of the peeled-off area of the ALD coatings

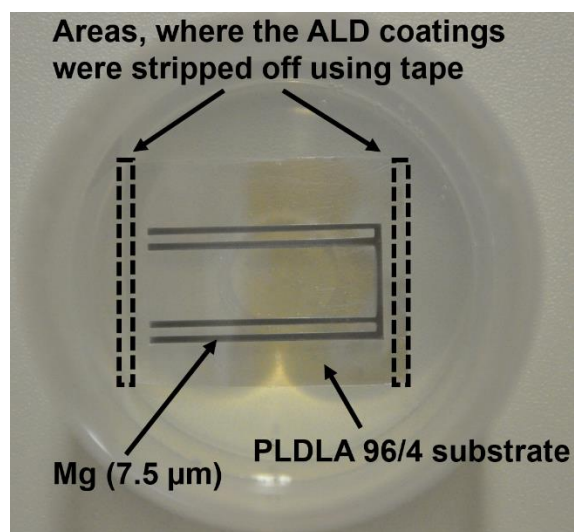


Figure S5. The image illustrates the areas, from where the ALD coatings were peeled off using tape. This was done to see the possible effects of water diffusion into the substrate.

8. ALD coated substrates in an LC resonator

LC resonators were formed using ALD coated (500 cycles or 50 nm) PLDLA 96/4 substrates (430 μm) with Mg conductors (7.5 μm) that were e-beam evaporated onto the ALD coatings as shown in Figure S6a. Two substrates were separated with a compression molded PLDLA 96/4 spacer (80 μm) and the whole structure was then melt welded from the sides. The resonator architecture was based on the design by Salpavaara et al. with the exception of the insulating polymer spacer instead of evaporated SiO_2 dielectric layers.⁷

The behavior of the resonator with ALD coated substrates under immersion (Sørensen buffer, +37 $^\circ\text{C}$) was similar to earlier reported non-coated resonators in the sense that the resonance frequency of the device started to increase steeply within the first 24 hours.^{7,8} In this case, after 10 hours of immersion, the resonance frequency of the sensor increased from less than 70 MHz to over 100 MHz in 1.5 hours. Furthermore, after 24 hours of immersion, the ALD coatings showed clear cracks (Figure S6c).

The increasing resonance frequency indicates that the polymer substrates have undergone dimensional changes and bended away from each other. This could have been due to their swelling, or due to H_2 generation inside the resonator caused by the corroding the Mg conductors. Thus, with this kind of resonator structure where the water is allowed to diffuse into the polymer matrix from the welded sides, the ALD coating did not provide benefits in terms of stable operation. Further studies where a complete resonator is ALD coated would be interesting, even though in practical implant applications their defect-free insertion might be challenging.

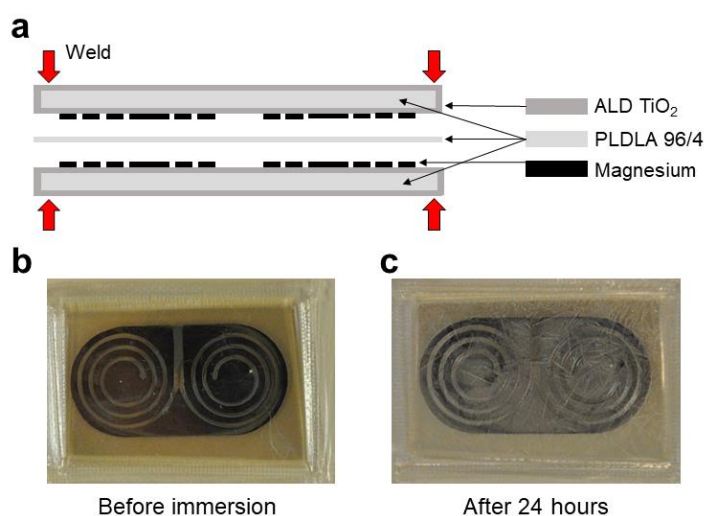


Figure S6. (a) Schematic image of the LC resonator structure, where the substrates were first ALD coated, then metallized and in the end heat sealed from the sides, as pointed by the red arrows. (b) A photograph of a resonator before immersion. (c) The resonator after 24 hours of immersion in Sørensen buffer solution, showing cracks in the ALD layer.

9. References

- (1) Ertel, S. I.; Kohn, J. Evaluation of a Series of Tyrosine-Derived Polycarbonates as Degradable Biomaterials. *J. Biomed. Mater. Res.* **1994**, 28 (8), 919–930. <https://doi.org/10.1002/jbm.820280811>.
- (2) Tirkkonen, L.; Halonen, H.; Hyttinen, J.; Kuokkanen, H.; Sievänen, H.; Koivisto, A.; Mannerström, B.; Sándor, G. K. B.; Suuronen, R.; Miettinen, S.; Haimi, S. The Effects of Vibration Loading on Adipose Stem Cell Number, Viability and Differentiation towards Bone-Forming Cells. *J. R. Soc. Interface* **2011**, 8 (65), 1736–1747. <https://doi.org/10.1098/rsif.2011.0211>.
- (3) Kueng, W.; Silber, E.; Eppenberger, U. Quantification of Cells Cultured on 96-Well Plates. *Anal. Biochem.* **1989**, 182 (1), 16–19. [https://doi.org/10.1016/0003-2697\(89\)90710-0](https://doi.org/10.1016/0003-2697(89)90710-0).
- (4) Miettinen, S.; Ahonen, M. H.; Lou, Y.-R.; Manninen, T.; Tuohimaa, P.; Syväälä, H.; Ylikomi, T. Role of 24-Hydroxylase in Vitamin D3 Growth Response of OVCAR-3 Ovarian Cancer Cells. *Int. J. Cancer* **2004**, 108 (3), 367–373. <https://doi.org/10.1002/ijc.11520>.
- (5) Shaltout, A. H.; Gregori, S. Conformal-Mapping Model for Estimating the Resistance of Polygonal Inductors. In *2016 IEEE International Symposium on Circuits and Systems (ISCAS)*; 2016; pp 1274–1277. <https://doi.org/10.1109/ISCAS.2016.7527480>.
- (6) Edwards, T. C.; Steer, M. B. Appendix B: Material Properties. In *Foundations for Microstrip Circuit Design*; Wiley Online Books; John Wiley & Sons, Ltd, 2016; pp 635–642. <https://doi.org/doi:10.1002/9781118936160.app2>.
- (7) Salpavaara, T.; Ellä, V.; Kellomäki, M.; Leikkala, J. Biodegradable Passive Resonance Sensor: Fabrication and Initial Testing. In *BIODEVICES 2015 - 8th International Conference on Biomedical Electronics and Devices*; SCITEPRESS, 2015; pp 127–131. <https://doi.org/10.5220/0005255901270131>.
- (8) Palmroth, A.; Salpavaara, T.; Leikkala, J.; Kellomäki, M. Fabrication and Characterization of a Wireless Bioresorbable Pressure Sensor. *Adv. Mater. Technol.* **2019**, 0 (0), 1900428. <https://doi.org/10.1002/admt.201900428>.